Journal Name

Dynamic Article Links ▶

Cite this: DOI: 10.1039/c0xx00000x

www.rsc.org/xxxxxx

ARTICLE TYPE

Carborane functionalization of the aromatic network in chemically-synthesized graphene

Jan U. Kahlert,[a] Aditya Rawal,[b] James M. Hook,[b] Louis M. Rendina*[a] and Mohammad Choucair*[a]

Received (in XXX, XXX) Xth XXXXXXXXX 20XX, Accepted Xth XXXXXXXXX 20XX

DOI: 10.1039/b000000x

The conjugated aromatic system of graphene was used to trap the reactive, boron-rich 1,2-carboryne cluster. Functionalization of the graphene surface was confirmed by solid-state MAS ^{11}B NMR spectroscopy and quantified by X-ray photoelectron spectroscopy. This work represents the first confirmed example of direct functionalization of a graphene lattice with carboranes.

New graphene materials require high thermal, oxidative, and chemical stabilities if they are to be utilized in nanotechnology.[1] Chemically-synthesised graphenes and chemically-treated graphene oxides are often employed in the preparation of functional graphene-based materials as they offer imperfect polar surfaces and secondary reactive sites capable of covalent and non-covalent chemical modification.[2-4] Chemical derivatization procedures have accessed the graphene lattice by reactions with radicals[5] and diazonium compounds.[6, 7] The boron cluster compound 1,2-carborane is a versatile building block for functional materials[8, 9] and has recently been appended to the surface functional groups of carbon nanotubes and graphene oxide resulting in materials with highly desirable physical and chemical properties.[10, 11]

In contrast, the ability to activate the pristine graphene lattice for further, more complex chemical reactions, such as those involving inorganic cluster compounds, is a considerable challenge.[12] To our knowledge, no report of the covalent attachment of a boron cluster directly to the graphene lattice has been made to date. Incorporating boron clusters directly onto the conducting and structurally robust graphene lattice would enable the development of exciting new graphene based hybrid materials as boron clusters are known to demonstrate strong supramolecular interactions with macrocyclic compounds[13, 14] and hydrophobic protein sites,[15] alter orbital energies of attached π-systems,[16] act as electron acceptors upon reduction[17] and photoexcitation,[18, 19] and can undergo further conversion to metallacarboranes.[8]

Herein we report the one-step covalent attachment of the reactive boron-rich 1,2-carborane cluster to the graphene lattice by a simple cycloaddition reaction. In contrast to reactions performed on highly oxidized graphene, we used bulk quantities of a chemically-synthesized graphitic material where the structural coherence between the layers is missing, approximating very well to an assembly of free graphene sheets that do not require any oxidative pre-treatments or post-synthetic surface activation.[20, 21]

Conversion of 1,2-carborane into the di-anion 1,2-dilithio-1,2-carborane was achieved by using two equivalents of *n*-butyllithium to deprotonate the slightly acidic C-H vertices of the precursor boron cluster.[22] The reaction of 1,2-dilithio-1,2-carborane with one equivalent of Br_2 resulted in the formation of 1-lithio-2-bromo-1,2-carborane. This species was only moderately stable at 0°C and elimination of LiBr occurred when warmed to ambient temperatures (*ca*. 30°C). The carborane product of this 1,2-elimination reaction, 1,2-dehydro-1,2-carborane, is usually referred to as '1,2-carboryne' due to its formal analogy with benzyne (1,2-dehydrobenzene). As found with benzyne, 1,2-carboryne is known to undergo [2+2] and [4+2] cycloaddition reactions with aromatic and unsaturated aliphatic hydrocarbons.[23] Similarly, the highly reactive boron cage in 1,2-carboryne was trapped by the arene network of the extended graphene sheets, to afford the new carborane-graphene material **1** (Scheme 1).

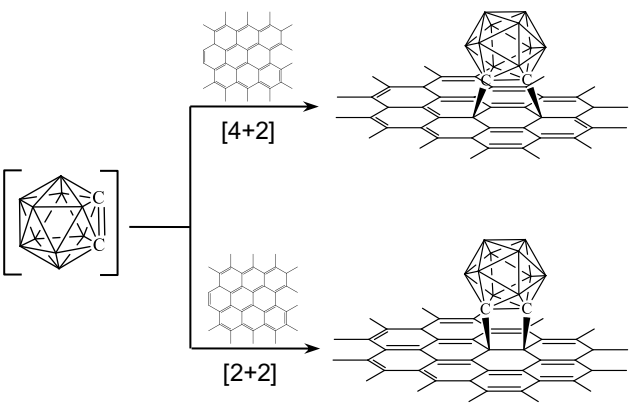

Scheme 1 Possible reaction pathways for graphene with 1,2-carboryne. Unlabelled carborane vertices represent BH groups.

Atomic force microscopy (AFM) and transmission electron microscopy (TEM) experiments confirmed the graphene sheets stack randomly with no interplanar correlation and the large-scale extended graphene structure was preserved after carborane functionalization (Fig. 1a and 1c, Supporting Information S2). AFM performed on **1** revealed the step height between the surface of overlapping sheets to be consistently 5 Å ± 1 Å,

confirming single atom-thick graphene layers with a low surface coverage of functional groups (Fig. 1b). The sheets in **1** retained a remarkable flatness; the root mean square roughness of the top layer graphene sheet in Fig. 1a was 1.3 Å ± 0.1 Å, comparable to the atomically smooth surface of the freshly cleaved mica substrate which had a root mean square roughness of 1.2 Å ± 0.1 Å. The flatness of the graphene surface in **1** allowed for relatively large individual molecular size features of 1–2 nm to be clearly distinguished at less than full monolayer coverage (Fig. 1d, Supporting Information S3). These surface features are comparable in size to the 1,2-carborane cluster vertex-to-vertex distance of *ca.* 1 nm,[24] and were not observed on the mica substrate or the neat graphene.[20]

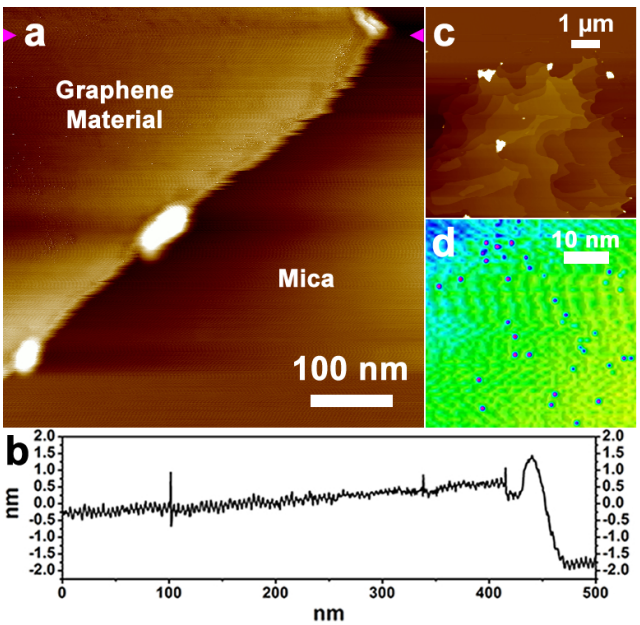

Fig. 1 (a) AFM topography image of the graphene material in **1** on a mica substrate with edge folding visible. (b) Height profile taken over the scan line indicated by arrows in (a) showing 5 Å ± 1 Å graphene layer on top of 5 to 6 layers. (c) Assembly of stacked graphene sheets in **1** extending over micron length scales. (d) Surface topography map of a flat graphene region in (a) showing carborane cluster sized surface features. The dark scattered 'spots' on the surface represent regions where the height profiles extend 1–2 nm upwards from the graphene surface.

The solid state ^{11}B NMR spectrum of **1** acquired at 30 kHz MAS at 224.7 MHz reveals, after subtraction of the probe-head background signal, peaks at -2.5 ppm and -13.5 ppm in Fig. 2a, readily assigned to the bound carborane cluster. The ^{11}B NMR chemical shifts were referenced using the 1,2-carborane as a secondary reference material (Fig. 2b).[25] A comparison of the spectra in Fig. 2a and 2b show similarities as well as significant differences.

Peaks in Fig. 2a closely match those in the neat 1,2-carborane, Fig. 2b, confirming the presence of the 1,2-carborane cage in the graphene material. It is important to note that the ^{11}B signals of the carborane in **1** are significantly broadened as compared to the signals of the neat 1,2-carborane, commensurate with the cluster now being locked onto the graphene surface and having its mobility 'frozen' in place. With neat 1,2-carborane, its high molecular symmetry and fast rotational dynamics serve to suppress the ^{11}B–^{11}B homonuclear, ^{11}B–^{1}H heteronuclear dipolar interactions, and the quadrupolar line broadening interaction. All these factors contribute to the very narrow spectral line-widths seen in the 30 kHz MAS NMR spectrum of neat 1,2-carborane. In comparison, the significant line broadening in the NMR spectrum of **1** can thus be attributed to the reduced rotational motions as well as a reduced symmetry in the molecule. These effects are consistent with the strong confinement of a somewhat less symmetrical derivative of 1,2-carborane, and with the covalent attachment of the carborane cage to the graphene surface.

It is important to note the low intensity of the ^{11}B NMR signals of **1** compared to those of the neat 1,2-carborane, as demonstrated by its significantly reduced signal-to-noise ratio. This low signal intensity indicates that a relatively small quantity of the carborane is attached to the graphene surface. After background subtraction, the distinct additional signal centered at 16.0 ppm can be attributed to the presence of oxidized boron, possibly B_2O_3, as found in borosilicate glass. This additional signal at 16.0 ppm is also observed in the graphene starting material (Supporting Information S4).

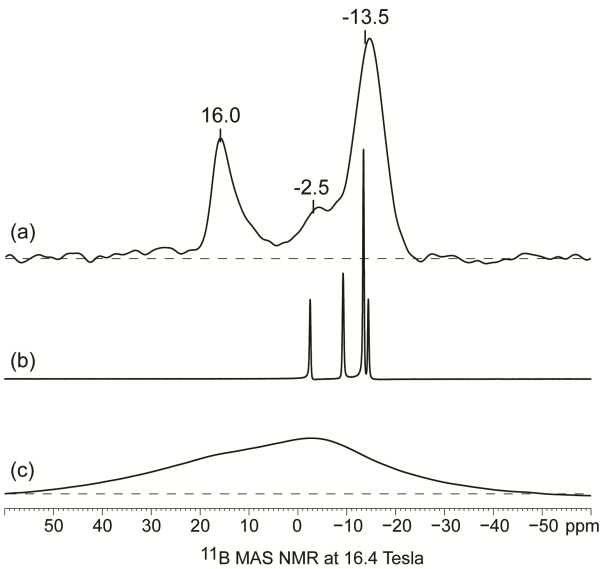

Fig. 2 Solid-state ^{11}B MAS NMR spectra of (a) **1**, dried under a dynamic vacuum at 120 °C for several hours (b) neat 1,2-carborane, and (c) the probe-head background signal. The spectra were acquired at 30 kHz MAS at room temperature, with a relaxation delay of 50 ms. Spectra (a) and (b) have been scaled to the same maximum intensity. Spectrum (c) is on the same intensity scale as (a) and reflects the intensity of the background signal relative to the signal of **1**.

X-ray photoelectron spectroscopy (XPS) was used to quantitatively examine the surface chemistry of **1** in order to establish the amount of carborane bound to its surface. Prior to analysis, **1** was dried under a dynamic vacuum at 120 °C for several hours to remove solvents and any residual unreacted 1,2-carborane. The elemental composition of **1** was resolved to distinguish the form of boron bound to the surface (Supporting Information S5). The corresponding in-depth analysis of the B 1*s* core line spectra confirmed a peak corresponding to the B–B/B–H binding energy of a carborane cluster at 189.4 eV (3.9 wt.%), and B in B_2O_3 (192.0 eV, 0.3 wt.%) from borosilicate glassware introduced during sonication.[26] The XPS data are consistent with the fact that the boron detected in **1** is covalently bound to the surface of graphene, well dispersed throughout the material, and

it could be readily distinguished from that of physisorbed 1,2-carborane on graphene materials prepared by simple solid- and solution-state mixing (Supporting Information S5). The atomic ratio of boron to carbon obtained from the XPS data indicate that approximately one carborane cage per 50 aromatic rings of graphene is bound to the surface.

Analysis of the X-ray photoelectron core C 1*s* line and Raman spectra of **1** identified an increase in the ratio of sp^3 to sp^2 carbon content compared to the neat graphene, consistent with the conversion of sp^2 to sp^3 carbons after functionalization (Supporting Information S6). No feature assignable to C–O–C bonding appeared in the Raman spectra between 830 to 930 cm^{-1}, consistent with the absence of bonding between the carborane and graphene by oxygen functional groups (Supporting Information S6).[27]

Differential charging of photoelectron lines in **1** by XPS confirmed that the carborane is electrically associated to the conducting graphene and that **1** is not electrically associated with the insulating borosilicate impurities (Supporting Information S7). Modulated temperature high resolution thermogravimetric analysis (mTGA) and *in-situ* variable temperature XPS measurements on **1** confirmed the slow removal of covalently-bound carborane, which remained bound to the graphene surface up to temperatures of 650 °C (Supporting Information S8).

Conclusions

We have demonstrated that the reactive boron cluster, 1,2-carboryne, can be trapped and remain covalently attached to the graphene surface by a simple one-step cycloaddition reaction. The low yield of functionalization obtained in this work parallels that of well-known carboryne trapping reactions involving smaller aromatic systems.[28] However, in order to apply this material to investigations on the nanoscale we are currently optimizing the reaction conditions to increase the amount of detectable boron clusters by other spectroscopic and microscopy characterization tools. Explorations of the mechanism of carborane cage attachment to the graphene surface remain unclear and are the subject of ongoing studies in our laboratories. The results of this work will be reported in due course.

Acknowledgements

MC and LMR acknowledge financial support from The University of Sydney and the ARC, respectively, and AFM support from Dr Chiara Neto and Mr Manuel Ghezzi.

Notes and references

[a] *School of Chemistry, The University of Sydney, Sydney 2006, Australia. E-mail: m.choucair@sydney.edu.au; E-mail: lou.rendina@sydney.edu.au*
[b] *Mark Wainwright Analytical Centre, NMR Facility, University of New South Wales, Sydney 2052, Australia.*

† Electronic Supplementary Information (ESI) available: Detailed experimental procedures, complete TEM, AFM, XPS, mTGA, and Raman characterization data. See DOI: 10.1039/b000000x/

1. D. Jariwala, V. K. Sangwan, L. J. Lauhon, T. J. Marks and M. C. Hersam, *Chemical Society Reviews*, 2013, **42**, 2824-2860.

2. D. Yu, Y. Hou and X. Wang, *Adv. Mater. Res. (Durnten-Zurich, Switz.)*, 2013, **788**, 3-6, 5 pp.

3. X. Huang, X. Qi, F. Boey and H. Zhang, *Chem. Soc. Rev.*, 2012, **41**, 666-686.

4. V. Georgakilas, M. Otyepka, A. B. Bourlinos, V. Chandra, N. Kim, K. C. Kemp, P. Hobza, R. Zboril and K. S. Kim, *Chemical Reviews*, 2012, **112**, 6156-6214.

5. H. Liu, S. Ryu, Z. Chen, M. L. Steigerwald, C. Nuckolls and L. E. Brus, *Journal of the American Chemical Society*, 2009, **131**, 17099-17101.

6. R. Sharma, J. H. Baik, C. J. Perera and M. S. Strano, *Nano Lett*, 2010, **10**, 398-405.

7. E. Bekyarova, M. E. Itkis, P. Ramesh, C. Berger, M. Sprinkle, W. A. de Heer and R. C. Haddon, *Journal of the American Chemical Society*, 2009, **131**, 1336-1337.

8. R. N. Grimes, *Carboranes*, 2nd edn., Academic Press (Elsevier), New York, 2011.

9. M. F. Hawthorne, *Comments on Inorganic Chemistry*, 2010, **31**, 153-163.

10. V. Stengl, S. Bakardjieva, M. Bakardjiev, B. Stibr and M. Kormunda, *Carbon*, 2014, **67**, 336-343.

11. Z. Yinghuai, A. T. Peng, K. Carpenter, J. A. Maguire, N. S. Hosmane and M. Takagaki, *J Am Chem Soc*, 2005, **127**, 9875-9880.

12. J. M. Englert, C. Dotzer, G. Yang, M. Schmid, C. Papp, J. M. Gottfried, H. P. Steinruck, E. Spiecker, F. Hauke and A. Hirsch, *Nat Chem*, 2011, **3**, 279-286.

13. H. Y. Ching, D. P. Buck, M. Bhadbhade, J. G. Collins and L. M. Rendina, *Chem Commun (Camb)*, 2012, **48**, 880-882.

14. C. L. Raston and G. W. Cave, *Chemistry*, 2004, **10**, 279-282.

15. F. Issa, M. Kassiou and L. M. Rendina, *Chemical reviews*, 2011, **111**, 5701-5722.

16. Y. Morisaki, M. Tominaga and Y. Chujo, *Chemistry*, 2012, **18**, 11251-11257.

17. J. Kahlert, H. G. Stammler, B. Neumann, R. A. Harder, L. Weber and M. A. Fox, *Angew Chem Int Ed Engl*, 2014.

18. L. Weber, J. Kahlert, R. Brockhinke, L. Böhling, A. Brockhinke, H. G. Stammler, B. Neumann, R. A. Harder and M. A. Fox, *Chem-Eur J*, 2012, **18**, 8347-8357.

19. K. R. Wee, Y. J. Cho, J. K. Song and S. O. Kang, *Angew Chem Int Ed Engl*, 2013, **52**, 9682-9685.

20. M. Choucair, P. Thordarson and J. A. Stride, *Nature Nanotechnology*, 2009, **4**, 30-33.

21. B. Náfrádi, M. Choucair and L. Forró, *Carbon*, 2014, **74**, 346-351.

22. M. A. Fox, in *Comprehensive Organometallic Chemistry III*, eds. R. H. Crabtree and D. M. P. Mingos, Elsevier, Oxford, 2007, vol. 3, pp. 49-112.

23. Z. Qiu and Z. Xie, *Dalton Trans*, 2014, **43**, 4925-4934.

24. M. G. Davidson, T. G. Hibbert, J. A. K. Howard, A. Mackinnon and K. Wade, *Chemical Communications*, 1996, 2285-2286.

25. R. K. Harris, J. Bowles, I. R. Stephenson and E. H. Wong, *Spectrochimica Acta Part A: Molecular Spectroscopy*, 1988, **44**, 273-276.

26. Y. Miura, H. Kusano, T. Nanba and S. Matsumoto, *Journal of Non-Crystalline Solids*, 2001, **290**, 1-14.

27. S. Sasic and Y. Ozaki, *Raman, infrared, and near-infrared chemical imaging*, John Wiley & Sons, Hoboken, New Jersey, 2011.

28. H. L. Gingrich, T. Ghosh, Q. Huang and M. Jones, *Journal of the American Chemical Society*, 1990, **112**, 4082-4083.